ELSEVIER

Three-dimensional model for multi-component reactive transport with variable density groundwater flow

X. Mao[a], H. Prommer[b], D.A. Barry[a,*], C.D. Langevin[c],
B. Panteleit[d], L. Li[e,f]

[a]Contaminated Land Assessment and Remediation Research Centre, Institute for Infrastructure and Environment,
School of Engineering and Electronics, King's Buildings, The University of Edinburgh, Edinburgh EH9 3JL, UK
[b]Department of Earth Sciences, Faculty of Geosciences, University of Utrecht, P.O. Box 80021, 3508 TA Utrecht,
The Netherlands and CSIRO Land and Water, Private Bag No. 5, Wembley WA 6913, Australia
[c]U.S. Geological Survey, STE 110 Miami, FL 33178, USA
[d]Geological Survey for Bremen, Friedrich-Missler-Strasse 46/50 28211 Bremen, Germany
[e]Centre for Eco-Environmental Modelling, Hohai University, Nanjing 210098, P R China
[f]Environmental Engineering Division, School of Engineering, The University of Queensland, St. Lucia,
QLD 4072, Australia

Abstract

PHWAT is a new model that couples a geochemical reaction model (PHREEQC-2) with a density-dependent groundwater flow and solute transport model (SEAWAT) using the split-operator approach. PHWAT was developed to simulate multi-component reactive transport in variable density groundwater flow. Fluid density in PHWAT depends not on only the concentration of a single species as in SEAWAT, but also the concentrations of other dissolved chemicals that can be subject to reactive processes. Simulation results of PHWAT and PHREEQC-2 were compared in their predictions of effluent concentration from a column experiment. Both models produced identical results, showing that PHWAT has correctly coupled the sub-packages. PHWAT was then applied to the simulation of a tank experiment in which seawater intrusion was accompanied by cation exchange. The density dependence of the intrusion and the snow-plough effect in the breakthrough curves were reflected in the model simulations, which were in good agreement with the measured breakthrough data. Comparison simulations that, in turn, excluded density effects and reactions allowed us to quantify the marked effect of ignoring these processes. Next, we explored numerical issues involved in the practical application of PHWAT using the example of a dense plume flowing into a tank containing fresh water. It was shown that PHWAT could model physically unstable flow and that numerical instabilities were suppressed. Physical instability developed in the model in accordance with the increase of the modified Rayleigh number for density-dependent flow, in agreement with previous research.
© 2004 Elsevier Ltd. All rights reserved.

Keywords: PHWAT; Density-dependent flow; SEAWAT; MODFLOW; MT3DMS; PHREEQC-2; Cation exchange; Seawater intrusion; Coastal groundwater flow and chemical transport/reaction; Snow-plough effect

* Corresponding author. Tel.: +44 131 650 7204; fax: +44 131 650 7276.

E-mail addresses: x.mao@ed.ac.uk (X. Mao), henning.prommer@csiro.au (H. Prommer), a.barry@ed.ac.uk (D.A. Barry), langevin@usgs.gov (C.D. Langevin), b.panteleit@nlfb.de (B. Panteleit), li_lingcj@hhu.edu.cn, l.li@uq.edu.au (L. Li).

Software availability

Name of software: PHWAT
Developers and contact addresses: X. Mao (first contact for software requests): Contaminated Land Assessment and Remediation Research Centre,

Institute for Infrastructure and Environment, School of Engineering and Electronics, King's Buildings, The University of Edinburgh, Edinburgh EH9 3JL, UK. Tel.: +44 131 650 5806; fax: +44 131 650 6781. E-mail: xmao@ed.ac.uk
H. Prommer: Department of Earth Sciences, Faculty of Geosciences, University of Utrecht, P.O. Box 80021, 3508 TA Utrecht, The Netherlands and CSIRO Land and Water, Private Bag No. 5, Wembley WA 6913, Australia. E-mail: henning.prommer@csiro.au
C.D. Langevin: U.S. Geological Survey, STE 110 Miami, FL 33178, USA. E-mail: langevin @usgs.gov

1. Introduction

In recent decades, groundwater resources have become increasingly threatened by the leaching of contaminants from uncontrolled landfills containing industrial and/or household waste, infiltration of pesticides and fertilizers from agricultural areas and leakage of a wide range of organic pollutants from petrol stations, refineries, pipelines (e.g., Trauth and Xanthopoulos, 1997; Anderson et al., 2000; Holt, 2000; Langwaldt and Puhakka, 2000; Johnson et al., 2001; Babiker et al., 2004; Quinn et al., 2004), etc., to name some of the most severe problems. In many circumstances, complex geochemical reactions, such as sorption, biodegradation, oxidation/reduction and precipitation/dissolution occur when contaminants enter the groundwater system and mix with the ambient water (e.g., Barry, 1992). Furthermore, saltwater intrusion degrades groundwater quality in many coastal areas, in most cases as a result of aquifer overuse (Mas-Pla et al., 1999; Ergil, 2000). Density variations play a key role in the dynamics of coastal aquifer hydrodynamics (e.g., Volker and Rushton, 1982; Bear et al., 1999; Kooi and Groen, 2001). Similarly, density differences between contaminant plumes and the ambient water might influence contaminant transport, particularly when instabilities develop and lead to increased spreading of contaminants or other groundwater constituents (Simmons and Narayan, 1998; Zhang et al., 2002).

Multi-component reactive transport models and variable density flow models are important tools for improving the understanding of governing processes in groundwater systems. Representatives of multi-component reactive transport models are, for example, MIN3P (Mayer, 1999), GIMRT/CRUNCH (Steefel, 2001), PHREEQC-II (Parkhurst et al., 1990; Parkhurst, 1995; Parkhurst and Appelo, 1999), PHAST (Parkhurst et al., 1995), HydroBioGeoChem (Yeh et al., 1998) and some MODFLOW/MT3DMS-based models such as RT3D (Clement et al., 1998) and PHT3D (Prommer et al., 2003). Numerous other models were developed for transport of a single solute species in aquifers with variable density, for example SUTRA (Voss, 1984), METROPOL (Sauter et al., 1993), FEMWATER (Lin et al., 1996), HST3D (Kipp, 1997), T3DVAP.F/ MOR3D.F (Bridwell and Travis, 1995), NAMMU (Herbert et al., 1988), FEFLOW (Kolditz et al., 1998) and MOCDENS3D (Oude Essink, 2001).

In a sizable proportion of cases the separation into the two problem classes (i.e., physical and reaction processes) is well justified because (i) density gradients are small enough to be of negligible influence on the reactive transport of multiple solutes or (ii) reactions, in particular water–sediment interactions such as mineral dissolution/precipitation and/or sorption, have only a minor effect on the density of the aqueous phase. However, situations exist where transport phenomena can only be accurately described by considering simultaneously both variable density and complex reactive processes. For example, simulation of the differential downward movement of a lithium and a bromide plume at Cape Cod required multi-component transport simulations that considered the variable density of the plume(s) and lithium sorption (Zhang et al., 1998). Furthermore, Christensen et al. (2001, 2002) demonstrated the interactions between reactive processes and density variations (i) for a controlled seawater intrusion experiment, where seawater was forced inland by pumping, thereby undergoing reactions such as Na/Ca exchange, calcite dissolution–precipitation, sulphate reduction and FeS precipitation, and (ii) for a landfill leachate plume, where the density influenced the distribution of redox-sensitive species and buffering reactions by Fe and Mn hydroxides.

Two major approaches are generally used to model such coupled processes, namely the one-step or global implicit approach (Zysset et al., 1994; Freedman and Ibaraki, 2002; Kanney et al., 2003a) and the sequential iteration or split-operator technique (Herzer and Kinzelbach, 1989; Yeh and Tripathi, 1989; Valocchi and Malmstead, 1992; Miller and Rabideau, 1993; Steefel and MacQuarrie, 1996; Barry et al., 1996a,b, 1997, 2000; Leeming et al., 1998; Prommer et al., 1999; Xu et al., 1999; Kanney et al., 2003b). The first

approach involves the simultaneous solution of a set of transport and chemical reaction equations. All reaction terms are inserted directly into the transport equations and result in a set of strongly non-linear equations. For example, Freedman and Ibaraki (2002) used this approach to develop a reactive transport model with variable density flow (DART). DART couples the existing code MITSU3D (Ibaraki, 1998) and GIMRT (Steefel and Yabusaki, 1996), and solves the non-linear equations using the Newton–Raphson method. In the second approach, the transport process and chemical reactions are de-coupled; transport is calculated first, followed by chemical reactions. Occasionally, iteration between the two steps (Yeh and Tripathi, 1989) is invoked in order to reduce numerical errors. The recent version of the geochemical reaction package PHREEQC-2 developed a one-dimensional reactive transport function based on this technique (Parkhurst and Appelo, 1999). A more detailed description of coupling procedures was, for example, given by Barry et al. (2002).

Until recently, the one-step or global implicit approach was generally considered to be less efficient due to the significantly higher demand for computer memory and relatively long execution time (Zhang and Schwartz, 1995). Considering the enormous advances in computer technology, this factor has become less important. Comparisons undertaken by Saaltink et al. (2001) have demonstrated that the efficiency of each approach can depend on the type of geochemical reactions and the number of nodes in the transport problem considered. Nevertheless, a major advantage of the split-operator approach is that existing and well-tested (sub)models that deal with individual physical or chemical processes can be combined relatively easily to solve the coupled problem (Walter et al., 1994; Pfingsten, 1996; Filius et al., 1999; Meeussen et al., 1999; Prommer et al., 1999, 2000, 2002). This approach has been adopted in the development of PHWAT.

Two existing models, the USGS density-dependent groundwater flow and solute transport model, SEA-WAT (Guo and Langevin, 2002), and the USGS geochemical reaction model, PHREEQC-2, were combined to create PHWAT. The SEAWAT code itself is a combination of two existing codes: the groundwater flow model MODFLOW-88 (McDonald and Harbaugh, 1988) and the multi-species transport model for saturated porous media, MT3DMS (Zheng and Wang, 1999). Both models were combined to enable the simulation of solute transport in flow-fields affected by variable density. The strategy adopted by PHWAT for coupling PHREEQC-2 and SEAWAT is similar to that used by the PHT3D model in combining PHREEQC-2 with the transport simulator MT3DMS (Prommer et al., 2003).

2. Model description

2.1. Governing equation for groundwater flow

Based on mass conservation, the governing equation for variable density groundwater flow in porous media is (e.g., Bear, 1979):

$$\frac{\partial(\rho\theta)}{\partial t} = -\nabla(\rho\vec{q}) + \overline{\rho}q_s, \tag{1}$$

where θ is the volumetric porosity, ρ [ML^{-3}] is the fluid density, $\overline{\rho}$[ML^{-3}] is the density of water entering from a source or leaving through a sink, q_s [T^{-1}] is the volumetric flow rate per unit volume of aquifer representing sources and sinks, t [T] is time and $\vec{q}$ [LT^{-1}] is the specific discharge vector (Darcy flux):

$$\vec{q} = \frac{-k}{\mu}(\nabla P - \rho g \nabla z), \tag{2}$$

where k [L^2] is the intrinsic permeability, μ [$ML^{-1}T^{-1}$] is the fluid dynamic viscosity, P [$ML^{-1}T^{-2}$] is fluid pore pressure, g [LT^{-2}] is the magnitude of gravitational acceleration and z [L] is the depth of a reference point to a datum. In SEAWAT, Eqs. (1) and (2) are reformulated in terms of equivalent freshwater head, which allows the constant density MODFLOW routines to solve for variable density groundwater flow with relatively few modifications (Guo and Langevin, 2002).

Under isothermal conditions, fluid density is a function of fluid pore pressure and solute concentrations in the solution, described as the as-yet-unspecified function (f):

$$\rho = f(P, C_1, C_2, \ldots, C_n), \tag{3}$$

where C_i [ML^{-3}] is the total concentration of the ith aqueous component and n is the total number of the dissolved components; here we use components to denote what is elsewhere termed master species (Parkhurst and Appelo, 1999). Therefore, we rewrite the left side of Eq. (1) as:

$$\frac{\partial(\rho\theta)}{\partial t} = \rho S_s \frac{\partial P}{\partial t} + \theta \sum_{i=1}^{n} \left(\frac{\partial\rho}{\partial C_i} \frac{\partial C_i}{\partial t} \right), \tag{4}$$

where S_s [$M^{-1}LT^2$] is the specific storage in terms of pressure, representing the volume of water released from storage in a unit volume of a confined elastic aquifer per unit change in pressure (e.g., Bear, 1979).

2.2. Governing equations for multi-component transport

The ith mobile aqueous component is transported in the groundwater by advection, molecular diffusion and mechanical dispersion. Simultaneously, each component is influenced by sources/sinks and/or geochemical

reactions. The governing equation is (e.g., Prommer et al., 2003):

$$\nabla(D\nabla C_i) - \nabla(\vec{v}\,C_i) - \frac{q_s}{\theta}C_{si} + \sum_{k=1}^{N} R_{k,i} = \frac{\partial C_i}{\partial t}. \tag{5}$$

For the ith immobile component, e.g., minerals, Eq. (5) simplifies to:

$$\frac{q_s}{\theta}C_{\mathrm{im}\,i} + \sum_{k=1}^{N} R_{k,i} = \frac{\partial C_{\mathrm{im}\,i}}{\partial t}. \tag{6}$$

In Eqs. (5) and (6), D [$L^2\,T^{-1}$] is the hydrodynamic dispersion coefficient (here assumed a scalar), $\vec{v}$ [LT^{-1}] is the fluid velocity, C_s [ML^{-3}] is the total aqueous component concentration in the water coming from sources or sinks, C_{im} [ML^{-3}] is the total concentration of the ith immobile component and $R_{k,i}$ ($k = 1, ..., N$) [$ML^{-3}T^{-1}$] is the rate of production or decay for component i in the kth reaction (of N different reactions undergone by this component).

For each component, the total concentration, C, is defined as (e.g., Prommer et al., 2003):

$$C = c_u + \sum_{i=1,n_s} Y_i^s s_i, \tag{7}$$

where c_u [ML^{-3}] is the concentration of the uncomplexed component, n_s is the number of dissolved species complexed with the aqueous component, Y_i^s is the stoichiometric coefficient of the component in the ith complexed species and s_i is the concentration of the ith complexed species. Redox state and pH are accounted for by simulating the transport of each redox state of a component separately and by a local charge balance condition, respectively.

2.3. Coupling between flow and transport in a groundwater system

Eq. (2) shows that the Darcy flux is influenced by the fluid density, which varies with the solute concentration.

The relationship between the density and the multicomponent concentration is complex due to the ionic interactions between the aqueous species (Monnin, 1989). Monnin (1994) developed a programme called VOPO that relates density to concentration based on Pitzer's ion-interaction model, which shows the error in the calculated seawater density is 0.00002 g/cm^3, and increases to about 0.0004 g/cm^3 for dense brines. We did not incorporate VOPO directly into our coupled model, but it is used to check an empirical linear relationship between density and concentrations. The latter relationship is used in the coupled model (Zhang and Schwartz, 1995; Simpson and Clement, 2003):

$$\rho = \rho_f + \sum_{i=1}^{n} \varepsilon_i C_i, \tag{8}$$

where ρ_f [ML^{-3}] is the density of freshwater and ε_i is a coefficient describing the influence of concentration of the ith component on the fluid density, i.e., ε_i is a density–concentration coupling term for each species considered.

The influence of density on the fluid dynamic viscosity μ is neglected in PHWAT as it is mainly influenced by temperature changes rather than the density variations considered here (Guo and Langevin, 2002). Temperature variations in the flow and transport simulations are not explicitly considered in the present version of PHWAT.

2.4. Reactions during solute transport

Both equilibrium and kinetic reactions can be modelled simultaneously in PHWAT. Where reactions are expected to proceed quickly relative to the transport (local equilibrium assumption), thermodynamically controlled equilibrium reactions are employed, based on the law of mass action (e.g., Stumm and Morgan, 1996; Schnoor, 1996). An example reaction can be written as:

$$aR_1 + bR_2 = cR_3 + dR_4. \tag{9}$$

The mass-action law requires:

$$K_{\mathrm{eq}} = \frac{[R_3]^c[R_4]^d}{[R_1]^a[R_2]^b}, \tag{10}$$

where a, b, c and d are the stoichiometric coefficients; R_1, R_2, R_3 and R_4 are the reactants and products, K_{eq} is the equilibrium constant and $[R_i]$ is the activity of species R_i.

When reactions proceed slowly relative to hydrodynamic transport, i.e., the local equilibrium assumption is violated, kinetically controlled reactions are employed. These are described mathematically as ordinary differential equations. The rate at which a product is generated is linked with the disappearance of a reactant. Many different formulations are possible; for example, Barry et al. (2002) describe approaches for modelling kinetically controlled microbial degradation of organic contaminants. In the coupled model, the set of user-defined kinetic reactions leads to a set of ordinary differential equations that are solved numerically within PHREEQC-2.

2.5. Structure of PHWAT

The structure of PHWAT is shown in Fig. 1. As mentioned above, PHWAT couples PHREEQC-2 with SEAWAT, which itself couples MODFLOW and MT3DMS. In PHWAT, the MODFLOW sub-package was further modified to relate the aqueous phase density
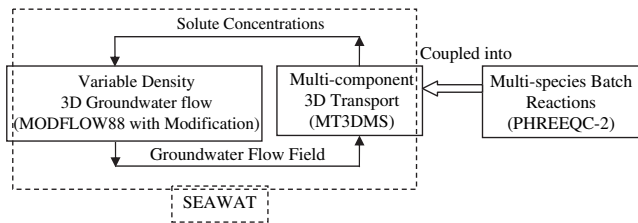
Fig. 1. Outline of model coupling used in PHWAT.

to all dissolved components instead of a single component.

For each time step, the following computations are carried out:

(1) The modified MODFLOW sub-package is used to simulate multi-component variable density groundwater flow. Chemical concentrations from the previous time step are used for calculating the spatially varying fluid density.
(2) The flow field and other related information are forwarded to the MT3DMS sub-package for simulation of multi-component chemical transport.
(3) The PHREEQC-2 geochemical speciation/reaction package is then called to simulate chemical reactions.

Iteration between steps (1) and (2) might be invoked to reduce the numerical error, as described by Guo and Langevin (2002).

3. Model evaluation

3.1. Evaluation of reactive transport

The reactive transport function in PHWAT was evaluated using experimental data on the elution of saline water by freshwater in a column filled with sandy sediments (Fig. 2). The experiment and its analysis were described in detail by Appelo et al. (1990) and Appelo (1994), and are recapped here briefly: the sediment was equilibrated with a salt solution containing the cations Na, Mg and Ca and the anion Cl and then flushed with fresh water to simulate the process of a freshwater injection into a brackish aquifer.

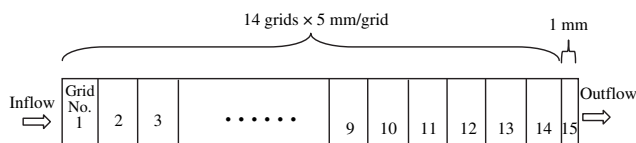The column length is 71 mm, with a sediment CEC (Cation Exchange Capacity) of 75 meq/l, where the

CEC units have been converted to litres of interstitial water (e.g., Bajracharya and Barry, 1995) obtained from an independent irrigation experiment using $SrCl_2$. The initial concentration of interstitial water and that of the water injected into the column are listed in Table 1. Ion-exchange reactions considered to occur during the experiment are shown in Table 2.

The experimental data were modelled with PHWAT and compared with the simulation results using the one-dimensional transport capability within PHREEQC-2.

Fig. 3 shows the simulation results of PHWAT and PHREEQC-2 and the observed leachate concentrations eluting the column. It is clear that the two simulation results are in close agreement, indicating that PHWAT has correctly coupled the component packages described earlier. The simulation predictions are in reasonable agreement with the experiment results. The differences mainly occur after leaching of about five pore volumes. This is likely caused by the exchange coefficients, which might in reality be slightly different in freshwater and saltwater but are treated as constants in the simulations.

3.2. Modelling of reactive transport under variable density conditions

3.2.1. Description of the tank experiment

Reactive transport and variable density flow were investigated in a laboratory-scale, sand-filled tank (Panteleit, 2004). The experimental design is shown in Fig. 4. The tank was nominally filled with three layers of soils. Each soil layer is assumed to be homogeneous and isotropic as the soil were thoroughly mixed before filling. The hydraulic conductivity, porosity and dispersivity are obtained from empirical experience and inverse modelling, as shown in Table 3 (the soil in layer 2 is the mixture of those in layers 1 and 3).

Artificial calcite-equilibrated groundwater was used as water inflow on the freshwater (left) side of the tank while the "seaside" (right side) contained seawater synthesized according to Grasshoff et al. (1999) (Table 4). Initially

Table 1
Solute concentrations of the interstitial water and the injected water

Water type	Na (mmol/l)	Mg (mmol/l)	Ca (mmol/l)	Cl (mmol/l)
Interstitial	110.0	5.0	0.966	121
Injected	1.05	0.99	3.17	9.37

Table 2
Ion-exchange reactions in the column

Formula of ion exchange	Log K[a]
$Na^+ + X^- = NaX$	0
$Mg^{2+} + 2X^- = MgX_2$	0.6
$Ca^{2+} + 2X^- = CaX_2$	0.8

[a] Values collected from PHREEQC-2 database.

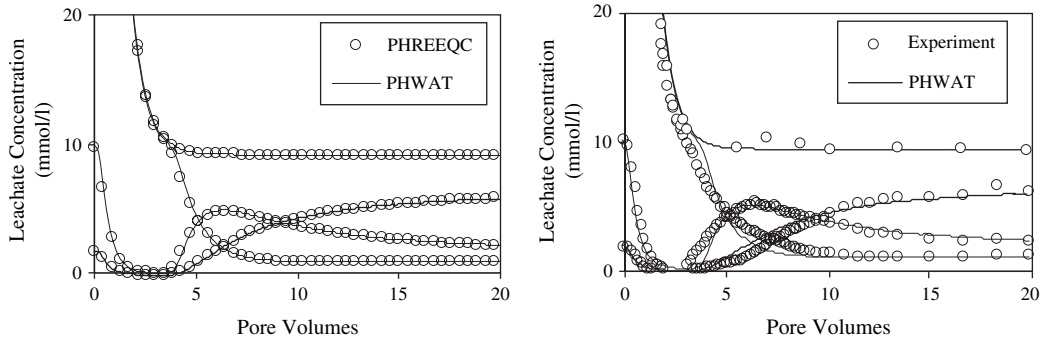Fig. 2. Physical conditions and simulation grid of the model domain.

Fig. 3. Simulation results by PHWAT and PHREEQC-2, and the experimental data showing effluent leachate concentrations.

the tank was filled with freshwater flowing from left to right with a hydraulic gradient of 0.003 at the free surface. Then the saltwater depth on the right boundary was raised stepwise replacing the freshwater from the bottom until it reached a thickness of 20 cm, which in total took several hours (Fig. 4). The experiment lasted for 3 d during which the vertical distribution of chemical components in the groundwater was measured every 7–9 h at the position 7.5 cm left of the "seaside" boundary.

3.2.2. Geochemical reactions and fluid density

Cation exchange is the main geochemical reaction during the experiment, while precipitation or dissolution reactions are assumed to be of negligible influence on the solute concentrations. The relevant cation exchange reactions included in the modelling and their reaction constants, listed in Table 2, were taken from the PHREEQC-2 database.

As can be seen from Table 4, the main ions influencing the water density are Cl, Na, SO_4, Mg, Ca, K and HCO_3. Therefore, the empirical coefficients describing the relationship between density and concentrations of these chemicals in Eq. (8) needed to be defined. For the present study, the parameters shown in

Table 5 were obtained from simulations using VOPO, which indicates that density is most sensitive to concentration variations of anions due to the effect of ion-interaction. Overall, the results from Eq. (8) agree well with the results from VOPO as well as with the experimental results (Ibaraki, 1998) (Fig. 5), showing that the model is valid over quite high concentrations.

3.2.3. Simulation results and discussion

PHWAT was used to simulate the seawater intrusion process in the experiment. Fig. 6 shows the velocity field and flow lines based on the simulated water head and concentration distributions at the end of the experiment. Fig. 7 shows the simulated Cl concentration contours in the tank at the same time. The flow lines show that the fresh water tends to flow upward as it approaches the outlet, while seawater intrudes into the lower portion of the tank, gradually rising until it flows out from the upper boundary. The simulation demonstrates that the density gradient has greatly influenced the hydrodynamic conditions; without the density influence, the flow lines would be nearly horizontal. The density-induced flow also influences the solute transport, as suggested by the high concentration of the conservative Cl ion (Fig. 7) in the lower portion of the tank.
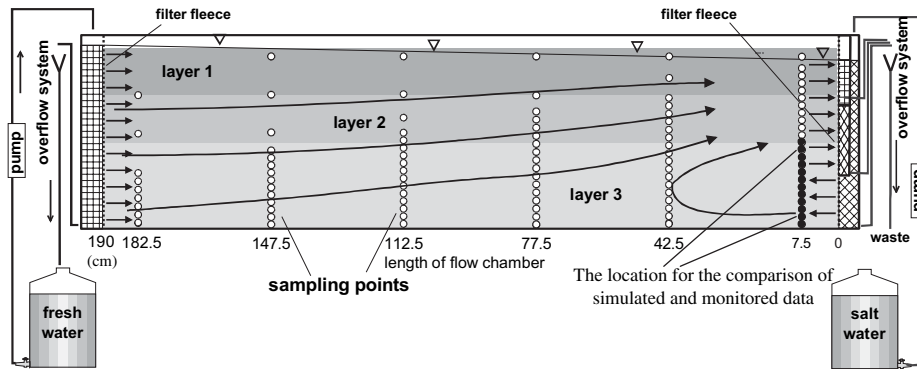

Fig. 4. Experimental set-up of the sand tank experiment (different shading represents different sediment types). Black circles indicate the positions where water samples were collected.

Table 3
Soil properties and hydrogeochemical parameters used as input for the simulation

Layer	Material	Soil water conductivity (m/s)	CEC (eq/l)	Porosity	Longitudinal dispersivity (m)[a]
1	Silt and clay	3.5×10^{-5}	0.4	0.40	0.005
2	Mixture of layer 1 and layer 3	7.1×10^{-4}	0.339	0.35	0.003
3	Fine sand–fine gravel	2.9×10^{-3}	0.278	0.30	0.001

[a] The values of horizontal and vertical transverse dispersivities are assumed to be the 10% of the longitudinal dispersivity.

Fluid density influences the transport of ions and chemical reactions influence the breakthrough curves. Fig. 8 shows the comparison of simulated and observed breakthrough curves of cation concentrations during the seawater intrusion. Two positions are shown in Fig. 4: the upper position is 7.5 cm to the left of the seawater boundary and 27 cm below the top of the tank; the lower position is 7.5 cm to the left of the seawater boundary and 45 cm below the top of the tank. The simulation results generally compare quite well with the measured concentrations. However, the simulated Ca concentration is slightly higher than that observed at the upper position. This deficiency is likely due to incomplete knowledge of hydraulic and hydrogeochemical properties. The results for Na, K and Mg show the same trends in their breakthrough curves; they increase steadily and tend to reach their maximum values after about 3 d. Ca shows a peak in the breakthrough, with the value much higher than that in the background freshwater and seawater. The peak is caused by a large amount of Ca exchanged from the soil into the soil water, where it is gradually flushing away during seawater intrusion. This phenomenon is known as the snow-plough effect and has been the subject of previous investigations (e.g., Starr and Parlange, 1979; Barry et al., 1983; Brooks et al., 1996).

In order to examine further the individual effect of reactions and variable density-influenced flow on the chemical transport, additional simulations were performed: (1) without considering the cation exchange reactions and (2) without considering the influence of variable density.

The comparison of simulated breakthrough curves for the cases with and without cation exchange reactions

Table 5
Coefficients for Eq. (8)

ρ_f (g/l)	ε_{Na} (g/mol)	ε_K (g/mol)	ε_{Ca} (g/mol)	ε_{Mg} (g/mol)	ε_{Cl} (g/mol)	ε_{SO_4} (g/mol)	ε_{HCO_3} (g/mol)
998.2	6	12.2	21.7	9.6	35.1	116.8	54.4

(both with density-influenced flow) are shown in Fig. 9. The concentrations of Na, K and Mg tend to be lower in the reactive case because the concentrations of these cations in seawater are 10–30 times higher than that in the freshwater. They tend to be absorbed onto the exchanger sites according to the mass-action law when seawater intrudes into the tank. As a result, the Ca is flushed from the exchanger sites into the water in the reactive case, resulting in a higher concentration of Ca compared to the non-reactive case.

For cases without density-influenced flow (Fig. 10), the simulated concentrations of all the cations were much lower than in the variable density case. Cation concentrations remain essentially unchanged in the absence of the intrusion of denser water. The simulation results shown in Figs. 9 and 10 demonstrate that PHWAT can not only suitably reflect the influence of the variable density and reactions on the chemical transport but also that it is necessary to consider both processes simultaneously in order to successfully reproduce the observed breakthrough curves.

4. Analysis of instabilities

4.1. Numerical instability induced by PHWAT

When mixed convective flow under variable density conditions is simulated, numerical models are susceptible to oscillations (Schincariol et al., 1994). It is difficult to distinguish these numerical instabilities from physical instabilities. Diersch and Kolditz (2002) discussed numerical issues for simulating the Elder (Elder, 1967) and salt lake (Simmons et al., 1999) problems. They found that standard numerical convergence could not be achieved at high Rayleigh numbers, i.e., the numerical results did not converge to a given configuration by using finer meshes. These findings demonstrate that simulating unstable flow from high density contrasts remains a numerically challenging problem. Therefore,

Table 4
Concentrations of ions in seawater and freshwater for the experiment

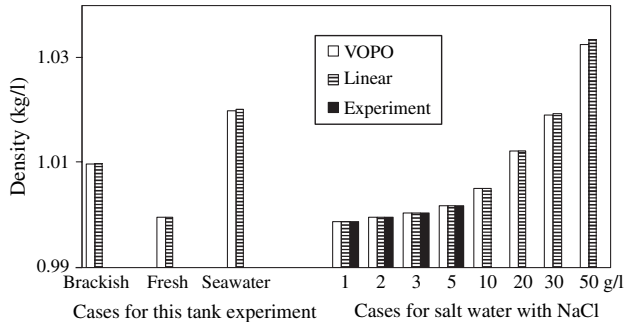| Water type	pH	HCO$_3$ (mg/l)	BO$_3$ (mg/l)	SO$_4$ (mg/l)	Cl (mg/l)	Na (mg/l)	Ca (mg/l)	K (mg/l)	Mg (mg/l)
Fresh water	7.93	17.74	0.07	639.82	1052.37	471.11	368.12	30.08	41.77
Seawater	7.95	24.67	0.01	2547.24	18 797.19	10 397.75	399.49	358.12	1159.15

Fig. 5. Comparison of density from the calculation using VOPO and the linear equation, together with experimental results.

we only evaluate PHWAT under low fluid density difference ranges, to investigate the occurrence of instabilities and to estimate the resulting errors. Simulations were conducted for a range of different spatial discretisation schemes and for different temporal step sizes by varying the Péclet number, Pe, and Courant number, Cr (Anderson and Woessner, 1992; Schincariol et al., 1994), respectively. These are defined as follows:

$$Pe = \frac{V\Delta l}{D} \tag{11}$$

and

$$Cr = \frac{V\Delta t}{\Delta l}, \tag{12}$$

where V [LT^{-1}] is the fluid velocity and Δl [L] and Δt [T] are grid size and time step, respectively. The effect of varying these quantities is discussed below.

The benchmark test involves the migration of a plume (NaCl) through a porous medium initially saturated with freshwater, as described by Ibaraki (1998). Note that Ibaraki's test was motivated by the experiments of Schincariol and Schwartz (1990). The schematic system design is shown in Fig. 11 and the relevant hydrogeological parameters are listed in Table 6.

Fig. 12 shows the result of concentration distribution from a 2000 mg/l source plume after migrating for 90 h
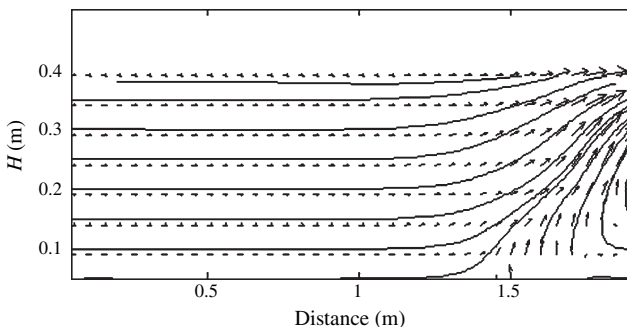

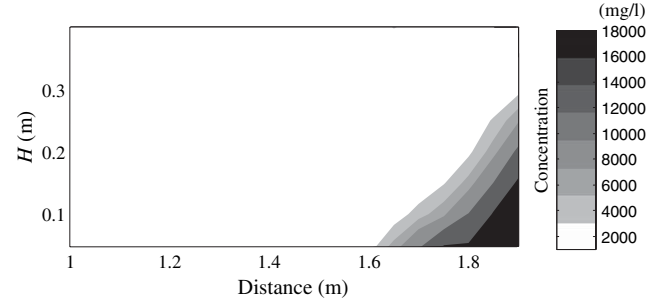Fig. 6. Streamlines in the tank after seawater intrusion for 3 d.

Fig. 7. Spatial distribution of Cl in the tank after seawater intrusion for 3 d.

with different grid sizes and time steps. For case (a), the grid size is 10 mm × 10 mm and the time step is 1 h, which give Pe as 11 and Cr as 1; for case (b), the grid size is 10 mm × 10 mm and the time step is 0.5 h, which give Pe as 11 and Cr as 0.5; for case (c), the grid size is 5 mm × 5 mm and the time step is 1 h, which give Pe as 5.5 and Cr as 2. There is a small but noticeable difference in results when the spatial step size is reduced (compare plots (a) and (c) in Fig. 12). The simulation with the small grid size shows the plume range reduces, indicating the effect of numerical dispersion. In contrast, the simulation results with different time steps are very similar because the packages in PHWAT will automatically divide the user-defined time step into smaller substeps to fulfil the appropriate stability criteria, thereby minimising numerical errors. Other errors would thus largely be associated with (temporal) operator splitting errors (e.g., Prommer et al., 2003), which increase with the length of the user-defined time step size. Therefore, the flow instability discussed in the following analysis is physical instability as modelled by the density-dependent model rather than numerically induced instability, given that it is within the low fluid density difference range used with similar physical configurations.

4.2. Instability development with different Rayleigh number

In simple free convective systems, the potential for instability is often characterised by the Rayleigh number (Ra), which is the ratio between buoyancy-driven forces and stabilising forces caused by diffusion and dispersion (e.g., Simmons et al., 2001):

$$Ra = \frac{gk(\rho_1 - \rho_2)H_0}{\theta \mu D_d}, \tag{13}$$

where D_d [L^{2}T^{-1}] is the hydrodynamic dispersion coefficient, ρ_1 [ML^{-3}] and ρ_2 [ML^{-3}] are the densities of the two fluids involved and H_0 is the thickness of the porous layer.
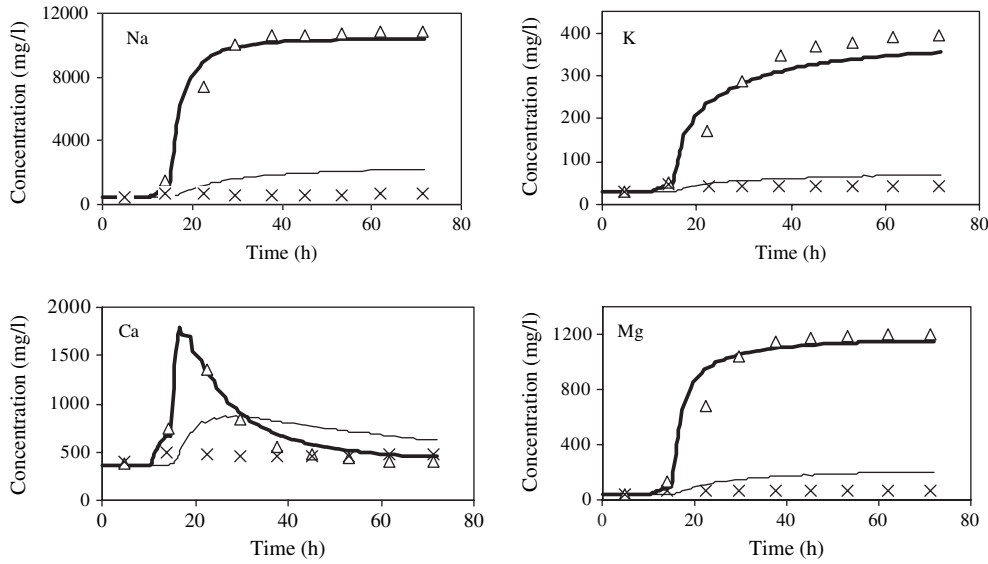
Fig. 8. Comparison of simulated and measured cation concentrations during seawater intrusion. Observation: × upper; △ lower. Simulation: — upper; — lower.

Simmons and Narayan (1997) use a modified Rayleigh number Ra^* and modified Péclet number Pe^* to account for the instability occurring in a saline disposal basin with solute-induced density-dependent flow:

$$Ra^* = \frac{Ra}{1 - Pe^*} \qquad (14)$$

and

$$Pe^* = \frac{V_{amb}\alpha_L}{D_0 + V_{amb}\alpha_L}, \qquad (15)$$

where V_{amb} [LT^{-1}] is the ambient velocity, α_L [L] is the longitudinal dispersivity and D_0 [L^{2}T^{-1}] is the molecular diffusion coefficient.

Based on the experiment mentioned in Section 4.1, numerical simulations were carried out with PHWAT to explore the development of physical instability with varying Ra^*. Fig. 13 shows simulation results for the 1000, 2000, 4000 mg/l NaCl source plumes flowing into the ambient fresh groundwater (the corresponding specific gravities are 1.00070, 1.00150 and 1.00291, giving respective Ra^* values of 734, 1467 and 2934). When the concentration was 1000 mg/l, the unstable "lobe" did not appear although at the front of the solute

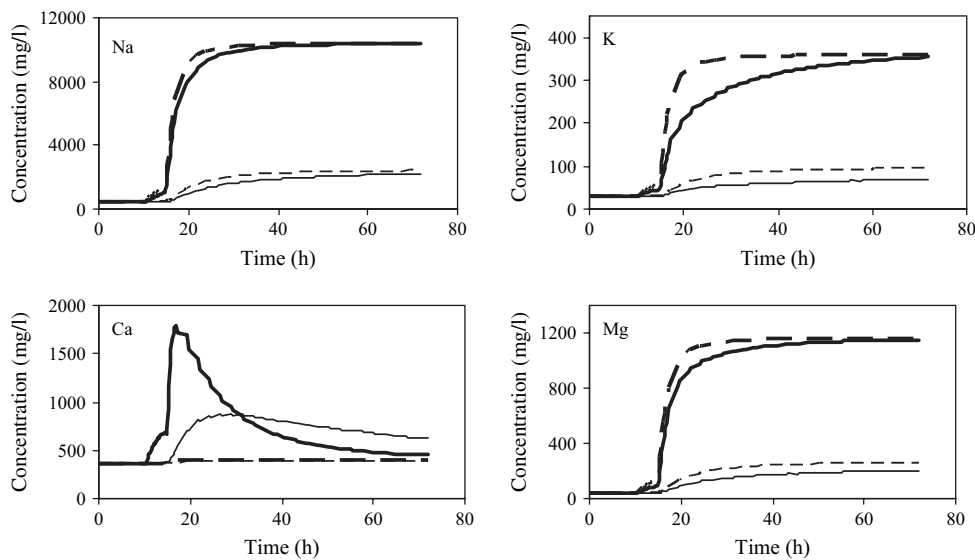

Fig. 9. Comparison of simulated cation concentrations for the cases with and without cation exchange. Without reaction: - - upper; -- lower. With reaction: — upper; — lower.
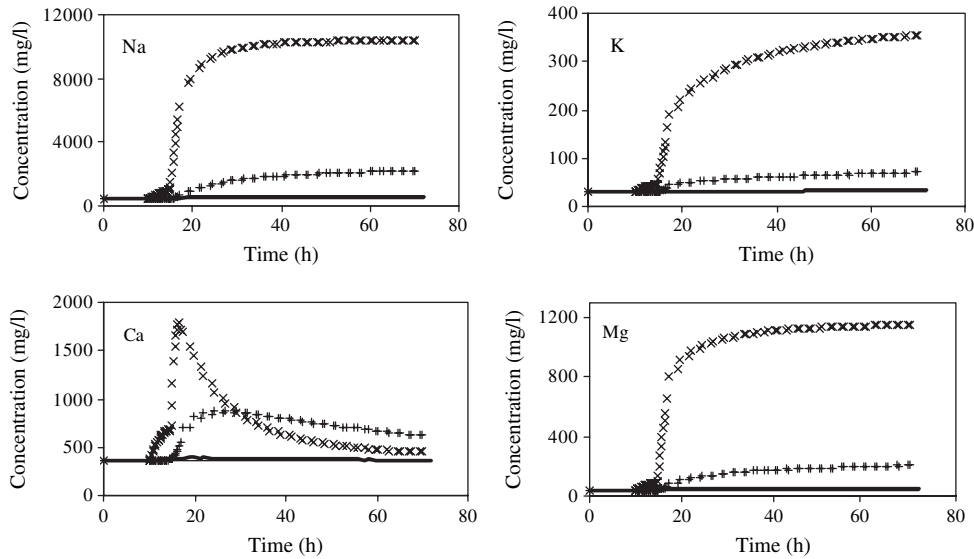
Fig. 10. Comparison of simulated breakthrough curves for the cases with and without density-influenced flow. Without density influence: — upper; — lower. With density influence: + upper; × lower.

plume the flow deviated slightly downward. When the concentration was increased to 2000 mg/l (with Ra^* of 1467), instability developed with one lobe appearing at the front of the plume. When the concentration was 4000 mg/l, the instability further developed with more than one lobe at the front part of the plume. These results are consistent with the instability criterion defined by Simmons and Narayan (1997, 1998): the flow remains stable until Ra^* exceeds 1250.

5. Concluding remarks

A three-dimensional model, PHWAT, has been developed to simulate multi-component reactive transport under variable density groundwater flow conditions. The coupling procedure of the newly developed model has initially been tested for a one-dimensional case of freshwater flushing into a soil column that is saturated with brackish water. Simulation results between PHWAT and PHREEQC-2 compare very well,

in which case we conclude that the PHREEQC-2 package has been correctly coupled with the flow and transport simulator SEAWAT. The combined model, of course, includes the modelling assumptions of the component models. The coupled model was then further applied to simulate a two-dimensional case of an experiment where seawater intrudes into a soil tank initially filled with freshwater. This experimental data set constitutes a new test for reactive transport models. The results demonstrate that the observations from the tank experiments can be reproduced only when both variable density flow and reactive processes are considered simultaneously. In this case the simulation results are in good agreement with the monitored data, indicating again that the coupled model is accurately representing the physical processes. Finally, a series of flow instability cases were studied with PHWAT. In those simulations a dense plume migrates into a tank filled with freshwater. The results demonstrate that PHWAT replicates the physical instability properly with instability developed with the increase of Ra^*, in agreement with previously published work.
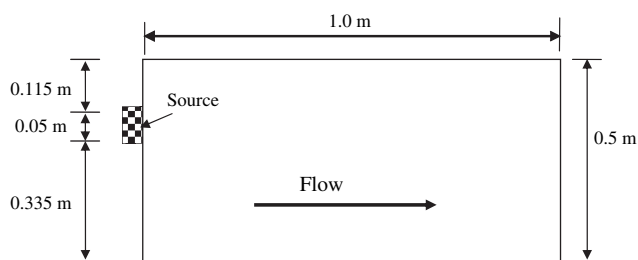

Fig. 11. Configuration of the model domain for instability analysis in PHWAT.

Table 6
Parameter values for numerical simulations

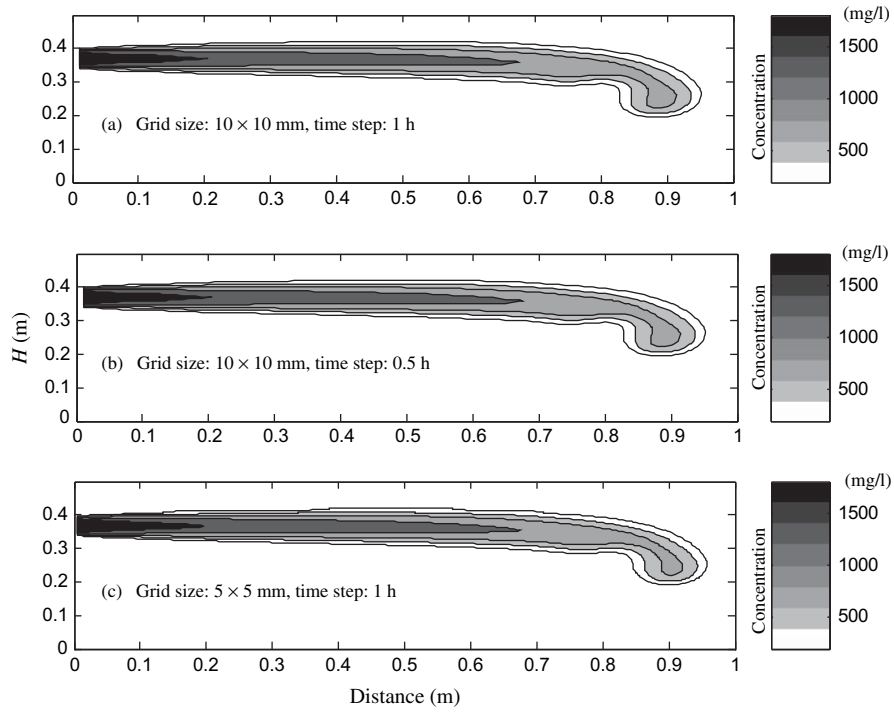| Parameter	Value
Permeability	5.7×10^{-11} m^2
Porosity	0.38
Free-solution diffusion coefficient	1.61×10^{-9} m^2/s
Average groundwater velocity	2.75×10^{-6} m/s
Longitudinal dispersivity	3.00×10^{-4} m
Transverse dispersivity	0.0 m

Fig. 12. Concentration distribution of a 2000 mg/l source plume after 90 h.

The reactions presented in this paper concern cation exchange; therefore additional work is needed to further verify PHWAT for other types of biogeochemical reactions. Future model development will include the interaction between biogeochemical reactions and hydrogeological properties, such as porosity and hydraulic conductivity. The modular design of PHWAT will allow one to quickly incorporate improved versions of the individual submodels. Possible model applications for PHWAT include in particular the field-scale
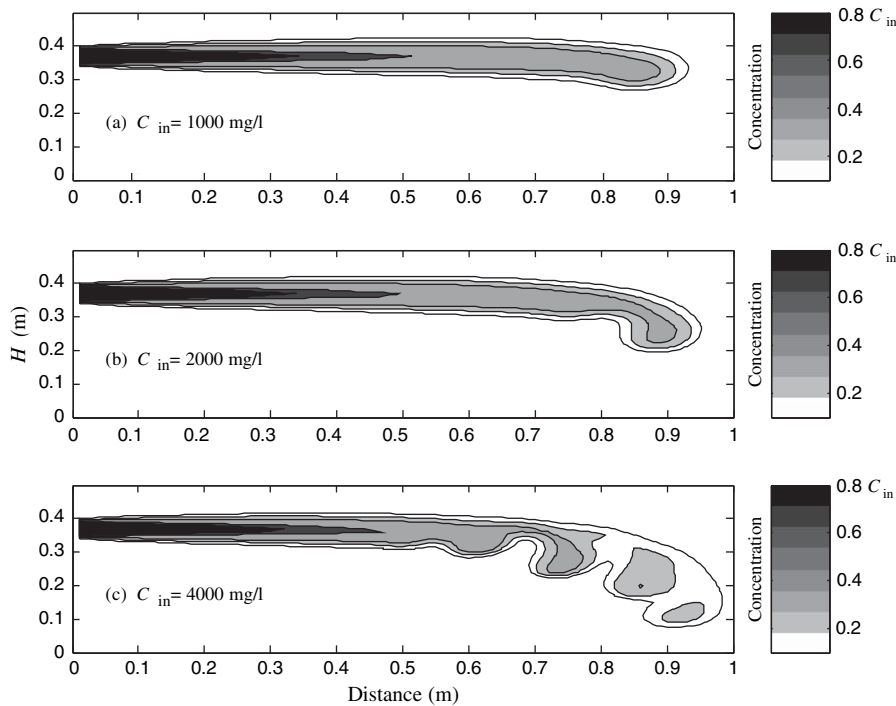

Fig. 13. Concentration distribution of NaCl with different incoming source plumes after 90 h.

simulation of the fate of organic and inorganic contaminants in subterranean coastal aquifers and the fate of dense plumes.

Acknowledgments

References

Anderson, M.A., Woessner, W.W., 1992. Applied Groundwater Modeling – Simulation of Flow and Advective Transport. Academic Press, Inc., San Diego, California, USA.

Anderson, P., Cunningham, C.J., Barry, D.A., 2000. Gravimetric analysis of organic contamination in railway ballast. Land Contamination and Reclamation 8 (2), 71–74.

Appelo, C.A.J., 1994. Cation and proton exchange, pH variations, and carbonate reactions in a freshening aquifer. Water Resources Research 30 (10), 2793–2805.

Appelo, C.A.J., Willemsen, A., Beekman, H.E., Griffioen, J., 1990. Geochemical calculations and observations on salt water intrusions, 2, validation of a geochemical model with column experiments. Journal of Hydrology 120 (1–4), 225–250.

Babiker, I.S., Mohamed, A.A.M., Terao, H., Kato, K., Ohta, K., 2004. Assessment of groundwater contamination by nitrate leaching from intensive vegetable cultivation using geographical information system. Environment International 29 (8), 1009–1017.

Bajracharya, K., Barry, D.A., 1995. Analysis of one-dimensional multispecies transport experiments in laboratory soil columns. Environment International 21 (5), 687–691.

Barry, D.A., 1992. Modelling contaminant transport in the subsurface: theory and computer programs. In: Ghadiri, H., Rose, C.W. (Eds.), Modelling Chemical Transport in Soil: Natural and Applied Contaminants. Lewis Publishers, Boca Raton, Florida, pp. 105–144.

Barry, D.A., Bajracharya, K., Crapper, M., Prommer, H., Cunningham, C.J., 2000. Comparison of split-operator methods for solving coupled chemical nonequilibrium reaction/groundwater transport models. Mathematics and Computers in Simulation 53 (1–2), 113–127.

Barry, D.A., Miller, C.T., Culligan, P.J., Bajracharya, K., 1997. Analysis of split operator methods for nonlinear and multispecies groundwater chemical transport models. Mathematics and Computers in Simulation 43 (3–6), 331–341.

Barry, D.A., Prommer, H., Miller, C.T., Engesgaard, P., Brun, A., Zheng, C., 2002. Modelling the fate of oxidisable organic contaminants in groundwater. Advances in Water Resources 25 (8–12), 945–983.

Barry, D.A., Starr, J.L., Parlange, J.-Y., Braddock, R.D., 1983. Numerical analysis of the snow-plow effect. Soil Science Society of America Journal 47 (5), 862–868.

Barry, D.A., Bajracharya, K., Miller, C.T., 1996a. Alternative split-operator approach for solving chemical reaction/groundwater transport models. Advances in Water Resources 19 (5), 261–275.

Barry, D.A., Miller, C.T., Culligan-Hensley, P.J., 1996b. Temporal discretisation errors in non-iterative split-operator approaches to solving chemical reaction groundwater transport models. Journal of Contaminant Hydrology 22 (1–2), 1–17.

Bear, J., 1979. Hydraulics of Groundwater. McGraw-Hill, New York, USA.

Bear, J., Cheng, A.H.-D., Sorec, S., Ouazar, D., Herrera, I., 1999. Seawater Intrusion in Coastal Aquifers – Concepts, Methods and Practices. Kluwer Academic Publishers, Dordrecht.

Bridwell, R.J., Travis, B.J., 1995. Numerical simulation of acid mine drainage (AMD) in a fully-coupled 3-D ground water flow and chemical transport model: Part I, field example and validation. In: Proceedings, Conference on Mining and the Environment, Sudbury, Ontario, Canada.

Brooks, S.C., Taylor, D.L., Jardine, P.M., 1996. Reactive transport of EDTA-complexed cobalt in the presence of ferrihydrite. Geochimica et Cosmochimica Acta 60 (11), 1899–1908.

Christensen, F.D., Basberg, L., Engesgaard, P., 2002. Modeling transport and biogeochemical processes in dense landfill leachate plumes. In: Hassanizadeh, S.M., Schotting, R.J., Gray, W.G., Pinder, G.F. (Eds.), Computational Methods in Water Resources, Proceedings of the XIV International Conference on Computational Methods in Water Resources (CMWR XIV). Elsevier, Amsterdam.

Christensen, F.D., Engesgaard, P., Kipp, K.L., 2001. A reactive transport investigation of seawater intrusion experiment in a shallow aquifer, Skansehage, Denmark. In: Proceedings of the First International Conference on Saltwater Intrusion and Coastal Aquifers, Essaouira, Morocco.

Clement, T.P., Sun, Y., Hooker, B.S., Petersen, J.N., 1998. Modeling multispecies reactive transport in ground water. Groundwater Monitoring and Remediation 18 (2), 79–92.

Diersch, H.-J.G., Kolditz, O., 2002. Variable-density flow and transport in porous media: approaches and challenges. Advances in Water Resources 25 (8–12), 899–944.

Elder, J.W., 1967. Steady free convection in a porous medium heated from below. Journal of Fluid Mechanics 27, 29–48.

Ergil, M.E., 2000. The salination problem of the Guzelyurt aquifer, Cyprus. Water Research 34 (4), 1201–1214.

Filius, J.D., Meeussen, J.C.L., van Riemsdijk, W.H., 1999. Transport of malonate in a goethite–silica sand system. Colloids and Surfaces. A, Physicochemical and Engineering Aspects 151 (1–2), 245–253.

Freedman, V.L., Ibaraki, M., 2002. Effects of chemical reactions on density-dependent fluid flow: on the numerical formulation and the development of instabilities. Advances in Water Resources 25 (4), 439–453.

Grasshoff, K., Kremling, K., Ehrhardt, M. (Eds.), 1999. Methods of Seawater Analysis. John Wiley & Sons, London.

Guo, W., Langevin, C.D., 2002. User's guide to SEAWAT: a computer program for simulation of three-dimensional variable-density ground-water flow. U.S. Geological Survey Techniques of Water-resources Investigations Book 6, USA.

Herbert, A.W., Jackson, C.P., Lever, D.A., 1988. Coupled groundwater flow and solute transport with fluid density strongly dependent on concentration. Water Resources Research 24 (10), 1781–1795.

Herzer, J., Kinzelbach, W., 1989. Coupling of transport and chemical processes in numerical transport models. Geoderma 44 (2–3), 115–127.

Holt, M.S., 2000. Sources of chemical contaminants and routes into the freshwater environment. Food and Chemical Toxicology 38 (Suppl.), S21–S27.

Ibaraki, M., 1998. A robust and efficient numerical model for analyses of density-dependent flow in porous media. Journal of Contaminant Hydrology 34 (3), 235–246.

Johnson, S.J., Barry, D.A., Christofi, N., Patel, D., 2001. Potential for anaerobic biodegradation of linear alkylbenzene cable oils:

literature review and preliminary investigation. Land Contamination and Reclamation 9 (3), 279–291.

Kanney, J.F., Miller, C.T., Barry, D.A., 2003a. Comparison of fully coupled approaches for approximating nonlinear transport and reaction problems. Advances in Water Resources 26 (4), 353–372.

Kanney, J.F., Miller, C.T., Kelley, C.T., 2003b. Convergence of iterative split-operator approaches for approximating nonlinear reactive transport problems. Advances in Water Resources 26 (3), 247–261.

Kipp Jr., K.L., 1997. Guide to the revised heat and solute transport simulator: HST3D Version 2. Water-resources Investigations Report 97-4157. U.S. Geological Survey, Colorado, USA.

Kolditz, O., Ratke, R., Diersch, H.-J., Zielke, W., 1998. Coupled groundwater flow and transport: 1. Verification of variable density flow and transport models. Advances in Water Resources 21 (1), 27–46.

Kooi, H., Groen, J., 2001. Offshore continuation of coastal groundwater systems: predictions using sharp-interface approximations and variable-density flow modelling. Journal of Hydrology 246 (1–4), 19–35.

Langwaldt, J.H., Puhakka, J.A., 2000. On-site biological remediation of contaminated groundwater: a review. Environmental Pollution 107 (2), 187–197.

Leeming, G.J.S., Mayer, K.U., Simpson, R.B., 1998. Effects of chemical reactions on iterative methods for implicit time stepping. Advances in Water Resources 22 (4), 333–347.

Lin, H.C., Richards, D.R., Yeh, G.T., Cheng, J.R., Cheng, H.P., Jones, N.L., 1996. FEMWATER: a three-dimensional finite element computer model for simulating density-dependent flow and transport. Technical report HL-96. US Army Engineer Waterways Experiment Station, USA.

Mas-Pla, J., Montaner, J., Solà, J., 1999. Groundwater resources and quality variations caused by gravel mining in coastal streams. Journal of Hydrology 216 (3–4), 197–213.

Mayer, K.U., 1999. A Numerical Model for Multicomponent Reactive Transport in Variably Saturated Porous Media. Ph.D. thesis, Department of Earth Sciences, University of Waterloo, Canada.

McDonald, M.G., Harbaugh, A.W., 1988. A Modular Three-Dimensional Finite-difference Ground-water Flow Model. U.S. Geological Survey, USA.

Meeussen, J.C.L., Kleikemper, J., Scheidegger, A.M., Borkovec, M., Paterson, E., van Riemsdijk, W.H., Sparks, D.L., 1999. Multicomponent transport of sulfate in a goethite-silica sand system at variable pH and ionic strength. Environmental Science and Technology 33 (19), 3443–3450.

Miller, C.T., Rabideau, A.J., 1993. Development of split-operator, Petrov–Galerkin methods to simulate transport and diffusion-problems. Water Resources Research 29 (7), 2227–2240.

Monnin, C., 1989. An ion interaction model for the volumetric properties of natural waters: density of the solution and partial modal volumes of electrolytes to high concentrations at $25\,^{\circ}C$. Geochimica et Cosmochimica Acta 53 (6), 1177–1188.

Monnin, C., 1994. Density calculation and concentration scale conversions for natural waters. Computers and Geosciences 20 (10), 1435–1445.

Oude Essink, G.H.P., 2001. Saltwater intrusion in 3D large-scale aquifers: a Dutch case. Physics and Chemistry of the Earth, Part B. Hydrology, Oceans and Atmosphere 26 (4), 337–344.

Panteleit, B., 2004. Geochemical Processes in the Salt–Freshwater Transition Zone, Reports of the Department of Earth Sciences, University Bremen, Nr. 225: Bremen, Germany.

Parkhurst, D.L., 1995. User's Guide to PHREEQC – a Computer Program for Speciation, Reaction-path, Advective-transport, and Inverse Geochemical Calculations. Investigations Report 95-4227. U.S. Geological Survey, USA.

Parkhurst, D.L., Appelo, C.A.J., 1999 (Version 2). User's Guide to PHREEQC – a Computer Program for Speciation, Reaction-path, 1D-transport, and Inverse Geochemical Calculations. Technical Report 99-4259. U.S. Geological Survey, USA.

Parkhurst, D.L., Engesgaard, P., Kipp, K.L., 1995. Coupling the geochemical model PHREEQC with a 3D multi-component solute transport model, paper presented at Fifth Annual V.M. Goldschmidt Conference. Geochemical Society, Penn State University, University Park, USA.

Parkhurst, D.L., Thorstenson, D.C., Plummer, L.N., 1990. PHREEQE – a computer program for geochemical calculations. U.S. Geological Survey Water-Resources Investigations Report 80-96, USA.

Pfingsten, W., 1996. Efficient modeling of reactive transport phenomena by a multispecies random walk coupled to chemical equilibrium. Nuclear Technology 116 (2), 208–221.

Prommer, H., Barry, D.A., Davis, G.B., 1999. A one-dimensional reactive multi-component transport model for biodegradation of petroleum hydrocarbons in groundwater. Environmental Modelling and Software 14 (2–3), 213–223.

Prommer, H., Barry, D.A., Davis, G.B., 2000. Numerical modelling for design and evaluation of groundwater remediation schemes. Ecological Modelling 128 (2–3), 181–195.

Prommer, H., Barry, D.A., Davis, G.B., 2002. Modelling of physical and reactive processes during biodegradation of a hydrocarbon plume under transient groundwater flow conditions. Journal of Contaminant Hydrology 59 (1–2), 113–131.

Prommer, H., Barry, D.A., Zheng, C., 2003. MODFLOW/MT3DMS-based reactive multicomponent transport modeling. Ground Water 41 (2), 247–257.

Quinn, N.W.T., Brekkeb, L.D., Millera, N.L., Heinzerc, T., Hidalgob, H., Dracup, J.A., 2004. Model integration for assessing future hydroclimate impacts on water resources, agricultural production and environmental quality in the San Joaquin Basin, California. Environmental Modelling and Software 19 (3), 305–316.

Saaltink, M.W., Carrera, J., Ayora, C., 2001. On the behavior of approaches to simulate reactive transport. Journal of Contaminant Hydrology 48 (3–4), 213–235.

Sauter, F.J., Leijnse, A., Beusen, A.H.W., 1993. METROPOL User's Guide, Report Number 725205003. National Institute of Public Health and Environmental Protection, Bilthoven, Netherlands.

Schincariol, R.A., Schwartz, F.W., 1990. An experimental investigation of variable density flow and mixing in homogeneous and heterogeneous media. Water Resources Research 26 (10), 2317–2329.

Schincariol, R.A., Schwartz, F.W., Mendoza, C.A., 1994. On the generation of instabilities in variable density flow. Water Resources Research 30 (4), 913–927.

Schnoor, J.L., 1996. Environmental Modelling: Fate and Transport of Pollutants in Water Air and Soil. John Wiley & Sons, New York, USA.

Simmons, C.T., Fenstemaker, T.R., Sharp, J.M., 2001. Variable-density groundwater flow and solute transport in heterogeneous porous media: approaches, resolutions and future challenges. Journal of Contaminant Hydrology 52 (1–4), 245–275.

Simmons, C.T., Narayan, K.A., 1997. Mixed convection processes below a saline disposal basin. Journal of Hydrology 194 (1–4), 263–285.

Simmons, C.T., Narayan, K.A., 1998. Modelling density-dependent flow and solute transport at the Lake Tutchewop saline disposal complex, Victoria. Journal of Hydrology 206 (3–4), 219–236.

Simmons, C.T., Narayan, K.A., Wooding, R.A., 1999. On a test case for density-dependent groundwater flow and solute transport models: the salt lake problem. Water Resources Research 35 (12), 3607–3620.

Simpson, M.J., Clement, T.P., 2003. Theoretical analysis of the worthiness of Henry and Elder problems as benchmarks of density-dependent groundwater flow models. Advances in Water Resources 26 (1), 17–31.

Starr, J.L., Parlange, J.-Y., 1979. Dispersion in soil columns – snow plow effect. Soil Science Society of America Journal 43 (3), 448–450.

Steefel, C.I., 2001. GIMRT, Version 1.2: Software for Modeling Multicomponent, Multidimensional Reactive Transport. User's Guide, UCRL-MA-143182. Lawrence Livermore National Laboratory, Livermore, California.

Steefel, C.I., MacQuarrie, K.T.B., 1996. Approaches to modeling of reactive transport in porous media. In: Lichtner, P.C., Steefel, C.I., Oelkers, E.H. (Eds.), Reviews in Mineralogy. Mineralogical Society of America, Washington.

Steefel, C.I., Yabusaki, S.B., 1996. OS3D/GIMRT: Software for Modelling Multicomponent–multidimensional Reactive Transport; User Manual and Programmer's Guide. Technical Report PNL-11166. Pacific Northwest National Laboratory, Richland, Washington.

Stumm, W., Morgan, J.J., 1996. Aquatic Chemistry. John Wiley & Sons, New York, USA.

Trauth, R., Xanthopoulos, C., 1997. Non-point pollution of groundwater in urban areas. Water Research 31 (11), 2711–2718.

Valocchi, A.J., Malmstead, M., 1992. Accuracy of operator splitting for advection–dispersion–reaction problems. Water Resources Research 28 (5), 1471–1476.

Volker, R.E., Rushton, K.R., 1982. An assessment of the importance of some parameters for seawater intrusion in aquifers and a comparison of dispersive and sharp-interface modelling approaches. Journal of Hydrology 6 (3–4), 239–250.

Voss, C.I., 1984. A finite-element simulation model for saturated–unsaturated, fluid-density-dependent ground-water flow with energy transport or chemically-reactive single-species solute transport. U.S. Geological Survey, USA.

Walter, A.L., Frind, E.O., Blowes, D.W., Ptacek, C.J., Molson, J.W., 1994. Modeling of multicomponent reactive transport in groundwater. 1. Model development and evaluation. Water Resources Research 30 (11), 3137–3148.

Xu, T.F., Samper, J., Ayora, C., Manzano, M., Custodio, E., 1999. Modeling of non-isothermal multi-component reactive transport in field scale porous media flow systems. Journal of Hydrology 214 (1–4), 144–164.

Yeh, G.T., Tripathi, V.S., 1989. A critical evaluation of recent developments of hydrogeochemical transport models of reactive multi-chemical components. Water Resources Research 25 (1), 93–108.

Yeh, G.T., Salvage, K.M., Gwo, J.P., Zachara, J.M., Szecsody, J.E., 1998. HYDROBIOGEOCHEM: a coupled model of HYDROlogic transport and mixed BIOGEOCHEMical kinetic/equilibrium reactions in saturated–unsaturated media. Oak Ridge National Laboratory, Center for Computational Sciences, Oak Ridge, USA.

Zhang, H., Schwartz, F.W., 1995. Multispecies contaminant plumes in variable density flow systems. Water Resources Research 31 (4), 837–848.

Zhang, H., Schwartz, F.W., Wood, W.W., Garabedian, S.P., LeBlanc, D.R., 1998. Simulation of variable-density flow and transport of reactive and non-reactive solutes during a tracer test at Cape Cod, Massachusetts. Water Resources Research 34 (1), 67–82.

Zhang, Q., Volker, R.E., Lockington, D.A., 2002. Experimental investigation of contaminant transport in coastal groundwater. Advances in Environmental Research 6 (3), 229–237.

Zheng, C., Wang, P.P., 1999. MT3DMS, a Modular Three-dimensional Multi-species Transport Model for Simulation of Advection, Dispersion and Chemical Reactions of Contaminants in Groundwater Systems; Documentation and User's Guide. U.S. Army Engineer Research and Development Center Contract Report SERDP-99-1, Vicksburg, USA.

Zysset, A., Stauffer, F., Dracos, T., 1994. Modeling of chemically reactive groundwater transport. Water Resources Research 30 (7), 2217–2228.